

**EXTENDED KALMAN FILTER BASED SOC ESTIMATION FOR EV
RANGE PREDICTION**

A DISSERTATION

Submitted by

SRAVAN PAI

(CB.EN.P2AEL17021)

in partial fulfillment for the award of the degree of

MASTER OF TECHNOLOGY

IN

AUTOMOTIVE ELECTRONICS



DEPARTMENT OF ELECTRONICS AND COMMUNICATION

ENGINEERING

AMRITA SCHOOL OF ENGINEERING

AMRITA VISHWA VIDYAPEETHAM

AMRITANAGAR, COIMBATORE - 641 112

JUNE 2019

ABSTRACT

Battery is the source of power for electric vehicles. Every battery at any instant has a capacity value known as state of charge (SoC) which reduces with energy usage. The health condition of the battery is obtained from SoH of the battery. Range of an EV depends on the SoC of the battery. Anxiety about drivable range, time required for charging and no information about battery SoH acts as a barrier for the acceptance of EV. Range of an EV depends on the route it travels which makes range prediction a bit difficult. This study proposes an improved method for SoC and drivable range prediction by considering environmental conditions of a location and other losses. SoC estimation being crucial in range prediction, is hence estimated using Extended Kalman Filter. The user gets to select the source and destination of the trip and SoC at the end of the trip is predicted.

TABLE OF CONTENTS

CONTENTS	PAGE NO.
ABSTRACT	i
LIST OF FIGURES	iv
LIST OF TABLES	vi
LIST OF ACRONYMS	x
1 INTRODUCTION	1
2 LITERATURE SURVEY	3
2.1 Introduction	3
2.2 Battery specifications – Nissan Leaf	3
2.3 Range prediction – Nissan Leaf	4
2.4 Range prediction – Tesla Model S	5
2.5 SoC estimation methods	7
2.6 Conclusion	8
3 POWER CONSUMPTION IN AN EV	9
3.1 Introduction	9
3.2 Power consumption along a user selected route	9
3.2.1 Tractive power consumption (P_{tra})	10
3.2.2 Inverter and Induction motor losses (P_{inv} and P_{ind})	11
3.2.3 Auxiliary load power consumption (P_{aux})	11
3.3 Conclusion	12
4 SoC ESTIMATION AND RANGE PREDICTION	13
4.1 Introduction	13
4.2 Thevenin battery model	13
4.3 Extended Kalman Filter algorithm	14

4.4	SoC estimation of the battery pack	18
4.5	Range estimation	18
4.6	Conclusion	20
5	SIMULATION AND EXPERIMENTAL RESULTS.....	21
5.1	System Overview	21
5.1.1	Range estimation block	21
5.1.2	EV parameters and system specifications.....	23
5.2	Simulation Results	23
5.2.1	Driving Scenario - 1	27
5.2.2	Driving Scenario - 2	27
5.2.3	Driving Scenario - 3	28
5.3	Hardware results.....	33
5.3.1	Design of PT	35
5.3.2	Design of CT	36
5.4	Conclusion	37
6	CONCLUSION AND FUTURE SCOPE	38
REFERENCES		39
PUBLICATIONS.....		42
APPENDIX A		43

LIST OF FIGURES

1.1	Block diagram of range estimation block	2
2.1	Battery module specifications.	3
2.2	Cell specifications.	4
2.3	Range chart for 24kWh battery.....	5
2.4	Range chart for 60kWh battery.....	5
2.5	Variation of SoC while trip.	6
2.6	Range and SoC display.....	6
2.7	Battery module specifications.	6
2.8	Tesla Model S performance specifications.	7
3.1	Power flow diagram in an EV.....	9
3.2	Total power consumption in an EV.	10
4.1	Thevenin battery model of a lithium-ion cell.	13
4.2	Terms related to state estimation.	15
4.3	Kalman Filter algorithm.	17
4.4	Representation of locations.	19
5.1	Range estimation block.	21
5.2	SoC estimation of Lithium-Ion cell using EKF.	24
5.3	Actual SoC vs Estimated SoC.	25
5.4	Error in SoC estimation.	25
5.5	Variation of voltage with SoC.	26
5.6	Current flowing through battery.	26
5.7	Simulation results of driving scenario - 1	27
5.8	Simulation results of driving scenario - 2	28

5.9	Simulation results of driving scenario - 3.....	29
5.10	Electric car trip statistics and drive information.....	29
5.11	Drive cycle vs Journey time.	30
5.12	Battery voltage vs Journey time.	30
5.13	Battery current vs Journey time.	31
5.14	Battery SoC vs Journey time.	31
5.15	Energy consumption vs Journey time.	32
5.16	Real time power vs Simulated power	32
5.17	Hardware setup.	33
5.18	Voltage transducer and Current transducer.....	33
5.19	Voltage transducer LV 20-P.....	36
5.20	Current transducer LA 25-NP.....	37

LIST OF TABLES

3.1	Tractive power components.....	11
3.2	Inverter and Induction motor losses.	11
3.3	Power consumed by auxiliary loads.	12
4.1	Driving scenarios.....	19
5.1	EV parameters and system specifications.	23

LIST OF SYMBOLS

ΔE	Energy consumed between destination and current locations
η_{trans}	Transmission efficiency
ω	Angular frequency
ρ_{air}	Density of air
A_f	Frontal area of the EV
Ah	Ampere Hour
C	Constant loss value
C_b	Bulk capacitance
C_d	Surface capacitance
C_{drag}	Drag coefficient
C_{r_eff}	Coefficient of rolling resistance
E	Energy available in battery
f_{swi}	Switching frequency
g	Acceleration due to gravity
I	Charging or discharging current
I_1	Primary current
I_2	Secondary current
I_Q	Switch current

k_1	Coefficient of proportional relation between torque and current
k_2	Added coefficient of friction and iron losses
k_3	Windage coefficient
K_k	Kalman gain
k_k	Elevation at the starting of segment k
m	Total mass of the EV
n	Number of turns per road segment obtained from Google Maps.
$P(\text{rain})$	Probability that it will rain
P_{cooling}	Power required for cooling
P_{heating}	Power required for heating
P_{wip}	Power consumed by wipers for working continuously
R_1	Resistance connected to primary
R_o	Output resistance
R_{CE}	On state resistance
R_d	Polarization resistance
R_i	Internal resistance
SoC	State of charge
SoH	State of health
T_{cabin}	Actual cabin temperature

$t_{off,sw}$	Turn off fall time
$t_{on,sw}$	Turn on rise time
T_{req}	Required cabin temperature
t_{seg}	Time taken for travelling between adjacent segments.
V	Voltage
V_{CE}	Voltage drop across the switch
V_{dr}	Drive cycle
V_{oc}	Open circuit voltage
V_o	Output voltage
V_{wind}	Velocity of wind

LIST OF ACRONYMS

AEC	Average energy consumption
AKF	Adaptive Kalman Filter
CT	Current transducer
EKF	Extended Kalman Filter
EV	Electric vehicle
KF	Kalman Filter
Li-Ion	Lithium-Ion
OCV	Open circuit voltage
PT	Potential transducer
SoC	State of charge
UKF	Unscented Kalman Filter

CHAPTER 1

INTRODUCTION

The range of an electric vehicle depends on the environmental conditions of the route, traffic existing in the route etc. Since EV batteries can't be recharged quickly, it creates stress and tension for the diver while journey, thinking whether he can reach the destination with the available SoC - especially while traveling at an odd time. Along with this, the batteries used in EV generally undergo a process known as self-discharge where the battery gets discharged even if the vehicle is not ON or it is not traveling. Because of this, the available SoC of the battery will reduce which may again create problem if there is no mechanism to alert the driver when the SoC goes less than minimum SoC limit. These problems may act as a barrier for the acceptance of EV. If a mechanism is available which notifies the driver the current SoC of the battery and the distance which can be travelled with this available SOC it will be of great help [1]. With this info the driver can check whether he can reach the destination without stop to charge or not.

In this study an improved method is proposed to estimate the state of charge of the battery and there by estimating the drivable range of the electric vehicle. Range of the electric vehicle can be observed as a function of battery SoC. So accurate estimation of SoC plays an important role in EV range prediction also. Accurate SoC estimation can be achieved by using Extended Kalman Filter algorithm (EKF). EKF is an optimal estimation algorithm which can be applied to any nonlinear systems. Since the battery model is nonlinear EKF can be used. A first order thevenin model is considered for deriving the state and measurement equations of the battery model. The range of an electric vehicle also depends on the energy it has consumed at the end of the trip. Figure 1.1 shows the overall block diagram of the range estimation block.

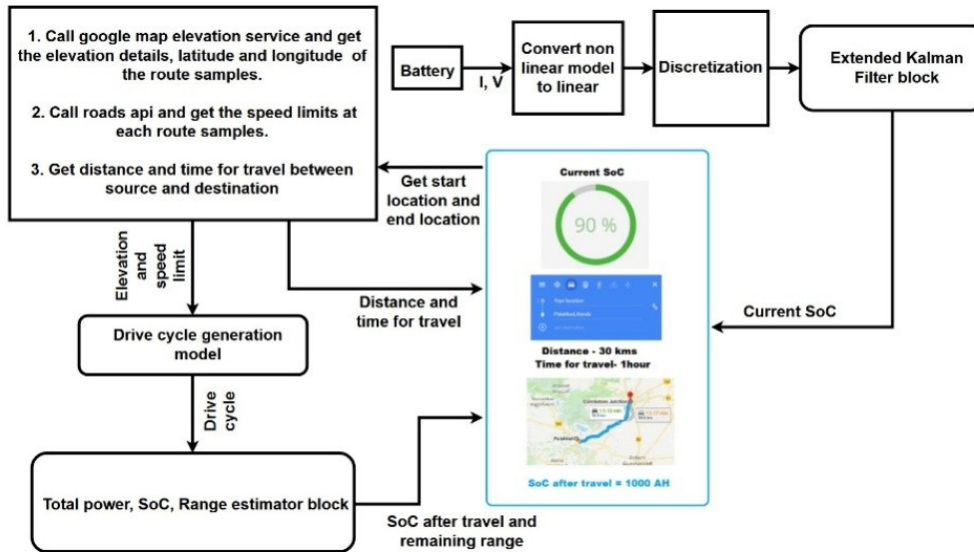


Figure 1.1: Block diagram of range estimation block.

Here every one second, the voltage across battery terminals and the current flowing through the battery are measured using sensors and given to the EKF block. Using these values and the battery model, the SoC of the battery is estimated and displayed in the dashboard as current SoC. The route that connects the source and destination is split into a number of route samples and the elevation details, latitude and longitude details of each of the samples is fetched via ElevationService - Google API call [2]. Roads API is also called to get the speed limits at the same route samples. Once all the required data is collected a drive cycle which the EV will have to follow at that particular time is predicted using a drive cycle generation model [3], [4]. Once the drive cycle is obtained the total power required to travel from source to destination, SoC at the destination and remaining range etc. are predicted and populated in the dashboard. The shortest distance between the source and the destination and the time required for the journey is taken directly from Google Maps as it is very precise. With the help of GPS data, nearby charging stations can be located and it can be notified to the driver [5]. The thesis is organized as 6 chapters, where the entire study is explained in detail with simulation results are validated using real time data. A hardware setup was also implemented which could measure the SoC of the battery accurately.

CHAPTER 2

LITERATURE SURVEY

2.1 Introduction

An extensive literature survey of SoC estimation methods and electric vehicle range estimation methods and are done in this chapter. The findings of this literature survey is also given in the upcoming chapters.

2.2 Battery specifications – Nissan Leaf

The nominal voltage and total capacity of the base Nissan Leaf model are **360V** and **24 kWh**. The battery modules specs and cell specs are given in Figure 2.1 and Figure 2.2 [6], [7].

Number of cells	4
Construction	2 in series pairs in parallel
Length	303mm
Width	223mm
Thickness	35mm
Weight	3.8kgs
Output terminal	M6 nut
Voltage sensing terminal	M4 nut

Figure 2.1: Battery module specifications.

Cell type	Laminate type
Cathode material	LiMn ₂ O ₄ with LiNiO ₂
Anode material	Graphite
Rated capacity (0.3C)	33.1AH
Average voltage	3.8V
Length	330mm
Width	216mm
Thickness	7.1mm
Weight	799g

Figure 2.2: Cell specifications.

2.3 Range prediction – Nissan Leaf

The Nissan Leaf is a compact electric car manufactured by Nissan in 2010 and introduced first in US and Japan. The driving range indicator in Nissan Leaf is known as ‘guess-o-meter’[6]. The guess-o-meter is noticed to be predicting range without considering road grade, aerodynamic drag, work done against rolling resistance, losses in motors/inverters and the auxiliary power requirements in the car. Hence the prediction can’t be said as an accurate one. Later prediction charts were introduced that can predict range better than the guess-o-meter. These charts vary depending upon battery capacity and battery degradation. In these charts also grade of road, weather conditions, power taken from auxiliary loads etc. are not considered. These charts were prepared for batteries with 24 kWh, 30 kWh and 60 kWh batteries. Multiple charts are available, out of them two charts are given in Figure 2.3 and Figure 2.4. [8]

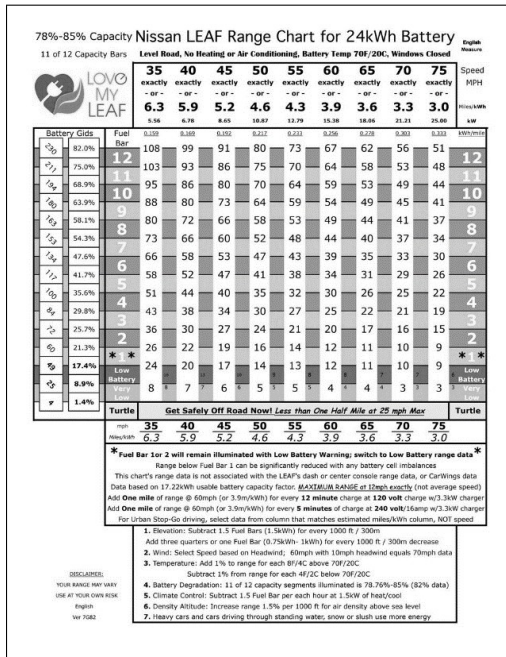


Figure 2.3: Range chart for 24kWh battery

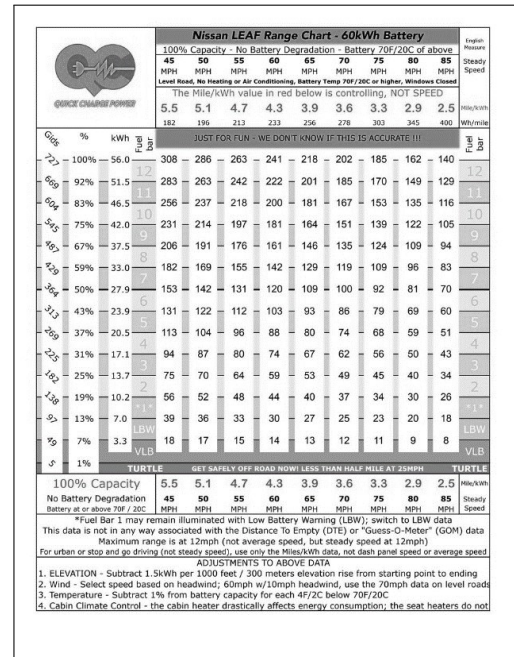


Figure 2.4: Range chart for 60kWh battery

2.4 Range prediction – Tesla Model S

The Tesla Model S is an all-electric car manufactured by Tesla, Inc. and introduced in 2012. In this car the range prediction is based on real time measurements of total energy consumption rate, road grade of the route, power consumption by auxiliary loads and the properties of drivetrain etc [9], [10]. Here the predicted range values are recalculated every 15-30 seconds thus promising accurate value of SoC and available driving range. Even during charging the predicted range and SoC are recalculated. But here the weather conditions of the route are not taken into consideration. Figure 2.5 and Figure 2.6 show the dash board display of pattern of battery discharge, current SoC and the SoC which will be left in the battery after the user defined trip. The nominal battery voltage of Tesla Model S is 375V. Battery energy and other specifications are given in Figure 2.7 and Figure 2.8 [11], [12], [13].

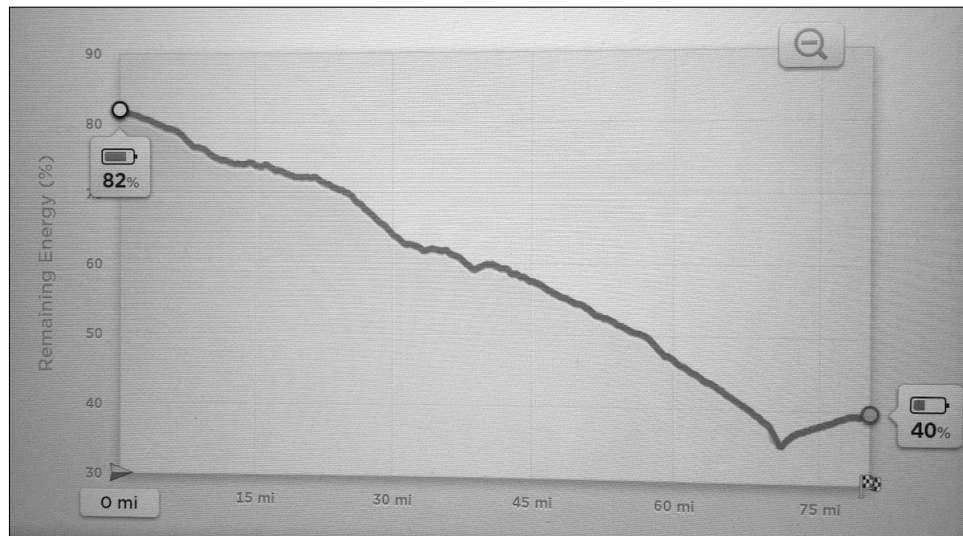


Figure 2.5: Variation of SoC while trip.

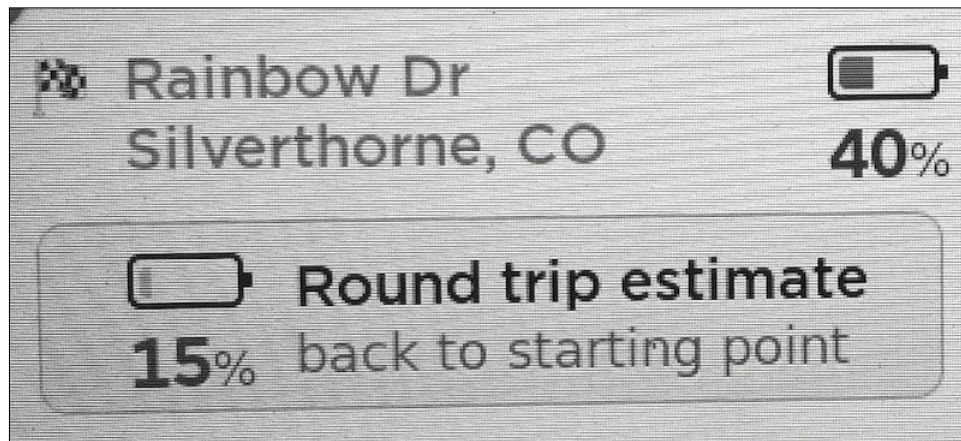


Figure 2.6: Range and SoC display.



Figure 2.7: Battery module specifications.

	60 kWh	85 kWh	85 kWh PERFORMANCE
Estimated Range at 55 mph	230 miles	300 miles	300 miles
EPA 5-Cycle Certified Range	208 miles	265 miles	265 miles
0 to 60 mph	5.9 seconds	5.4 seconds	4.2 seconds
Quarter Mile Time	14.2 seconds	13.7 seconds	12.6 seconds
Top Speed	120 mph	125 mph	130 mph
Peak Motor Power	302 hp (225 kW) 5,000-8,000 rpm	362 hp (270 kW) 6,000-9,500 rpm	416 hp (310 kW) 5,000-8,600 rpm
Peak Motor Torque	317 lb-ft (430 Nm) 0-5,000 rpm	325 lb-ft (440 Nm) 0-5,800 rpm	443 lb-ft (600 Nm) 0-5,100 rpm
Energy Storage	60 kWh	85 kWh	85 kWh
Battery Warranty	8 years, 125,000 miles	8 years, unlimited miles	8 years, unlimited miles
Supercharging	Optional	Included	Included
Enters Production	In Production	In Production	In Production

Figure 2.8: Tesla Model S performance specifications.

2.5 SoC estimation methods

SoC or state of charge is the percentage of total battery capacity available in the EV battey, which can be used to drive the vehicle. Estimation of SoC is very important, as it is essential that the driver should be aware of the state of the battery. Due of self-discharge and any other issues, the battery may drain fast and it is not appreciable if the driver is not notified of this.

A plenty of SoC estimation algorithms are available. Some of them are listed below.

- Ah counting method
- Open circuit voltage method (OCV)
- Impedance & internal resistance method
- Electrochemical method
- Extended Kalman Filter (EKF)
- Unscented Kalman Filter (UKF)
- Neural networks

In Ah counting method, the amount of current passing through the battery is measured with respect to time and it is decreased from the initial SoC when the battery is discharging and increased when the battery is charging. In OCV method, a relation between SoC of the battery and OCV is derived, so that at any value of voltage the SoC can be estimated. For the above said methods, the computation and calculations are very simple but the estimated SoC value may not be precise. Therefore, model based methods like EKF, UKF, neural networks etc. are used. These methods include calculations which are a bit complex, but the estimated SoC values has a high level of accuracy.

2.6 Conclusion

This chapter deals with SoC and range estimation methods available as of now. Below mentioned are the points obtained from literature survey.

- EV range estimation methods are available that predicts the range based on battery SoC, road parameters, environmental conditions.
- Accurate measurement of SoC plays a major role in range estimation.
- Extended and Unscented Kalman filters are available which estimates SoC with high accuracy.
- Battery model parameters vary with temperature and SoC.
- Relation between kinematic parameters of vehicle and energy consumption.
- Combining history-based and trip-based model gives a more accurate model with a high level of accuracy.

CHAPTER 3

POWER CONSUMPTION IN AN EV

3.1 Introduction

This chapter discusses about the total power consumption in an EV when it travels in a route defined or inputted by the user. The dashboard of the EV consists of a user interface to enter the source and destination details of the trip. Once these are entered in backend the total power consumption is calculated. Figure 3.1 [14] represents the power flow diagram in an EV. Power calculations and the power components involved etc. are discussed in the below sections.

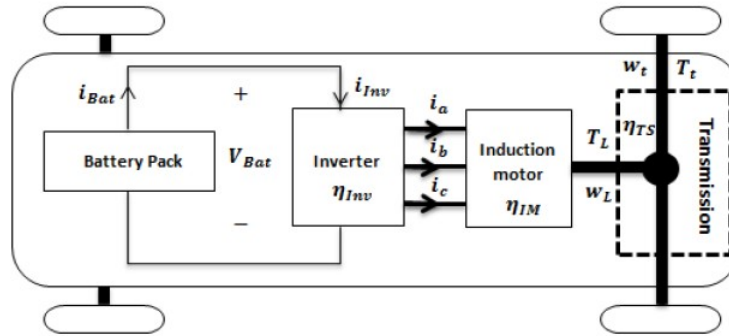


Figure 3.1: Power flow diagram in an EV.

3.2 Power consumption along a user selected route

The power consumed by an EV depends on environmental conditions of the route, traffic existing in the route, power used by auxiliary load etc. In this chapter the different power components that constitutes power consumption, the related equations and the variables involved are introduced [15], [16]. The total power consumption is constituted by the three major components namely tractive power consumption, inverter and induction machine losses and auxiliary power consumption. Figure 3.2 [17] gives a brief idea on these and the variables involved in calculating them.

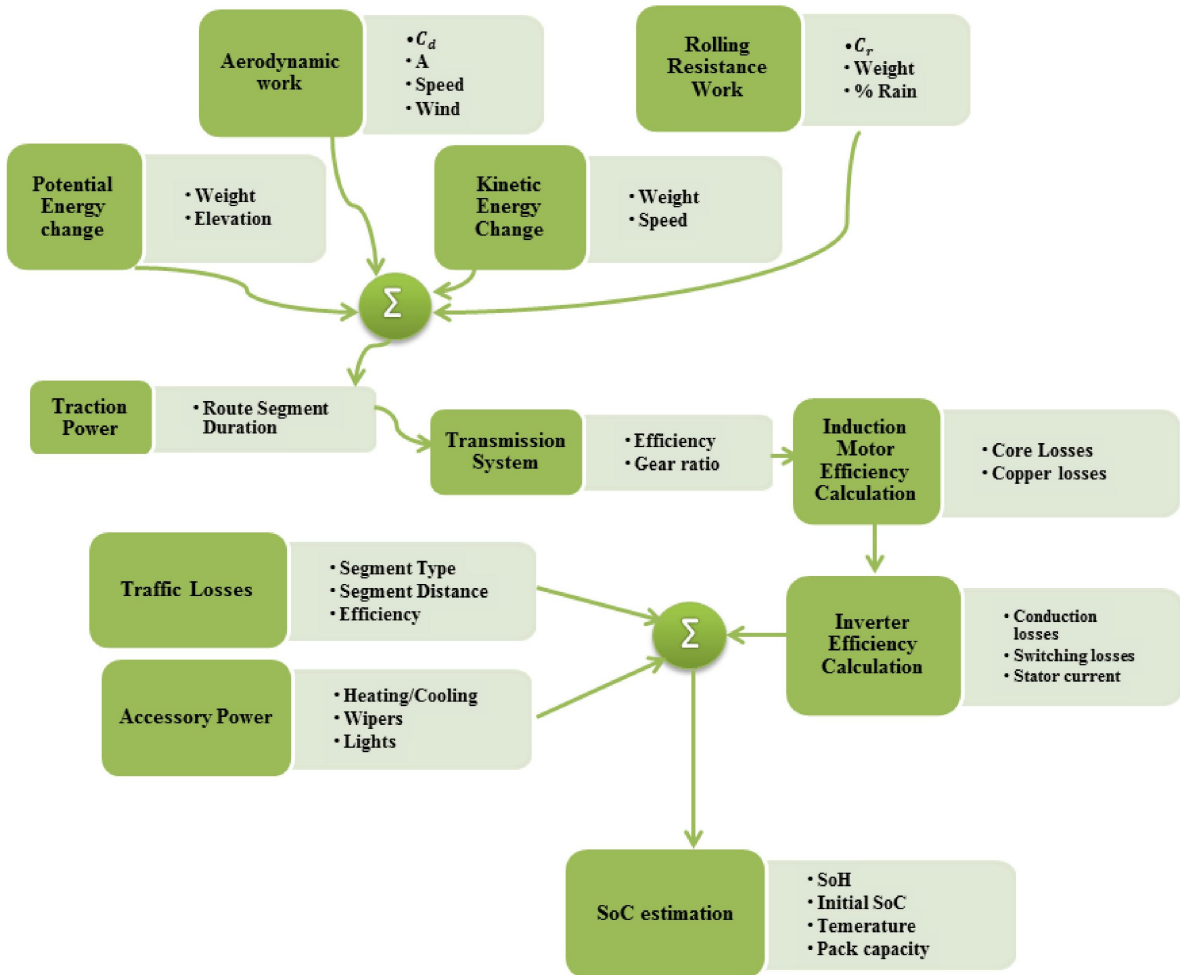


Figure 3.2: Total power consumption in an EV.

In the coming sections each of the above components are discussed in detail.

3.2.1 Tractive power consumption (P_{tra})

The tractive power consumption consists of work done against aerodynamic drag, work done against rolling resistance, change in potential energy and change in kinetic energy along the route of travel. The equations to calculate these components and the variables involved are given in the below Table 3.1.

Table 3.1: Tractive power components.

Power component (kW)	Equation
Power to overcome rolling resistance (P_{roll})	$P_{roll} = mgC_{r_eff}V_{dr}$
Power to overcome aerodynamic drag (P_{aero})	$P_{aero} = 0.5\rho_{air}C_{drag}A_f(V_{dr} + V_{wind})^2V_{dr}$
Power associated with change in potential energy (P_{PE})	$P_{PE} = \frac{1}{t_{seg}}mg(h_k - h_{k-1})$
Power associated with change in kinetic energy (P_{KE})	$P_{KE} = \frac{1}{2t_{seg}}m(v_{dr,k}^2 - v_{dr,k-1}^2)$
Total tractive power	$P_{tra} = (P_{roll} + P_{aero} + P_{PE} + P_{KE})\frac{1}{\eta_{trans}}$

3.2.2 Inverter and Induction motor losses (P_{inv} and P_{ind})

Whenever the EV is following a particular drive cycle, the voltage available across the motor terminals needs to be varied along with other control logics or algorithms. For getting variable voltages, the inverter switches have to be turned ON and OFF continuously, which may result in switching losses. The motor being an electric machine, will also contribute to copper losses and core losses. The equations to calculate these loss components are given in the Table 3.2.

Table 3.2: Inverter and Induction motor losses.

Loss component (kW)	Equation
Inverter losses (P_{inv})	$P_{inv} = P_{conduction} + P_{switching}$ $P_{conduction} = V_{CE}I_{Q,avg} + R_{CE,on}I_{Q,rms}^2$ $P_{switching} = \frac{1}{2}V_QI_Qf_{swi}(t_{on,sw} + t_{off,sw})$
Induction motor losses (P_{ind})	$P_{ind} = k_1T^2 + k_2\omega + k_3\omega^3 + C$

3.2.3 Auxiliary load power consumption (P_{aux})

The power consumed by auxiliary loads in an EV may contribute to auxiliary load power consumption. The most important auxiliary power requirements in an EV and the equations to compute

those are given in Table 3.3.

Table 3.3: Power consumed by auxiliary loads.

Power component (kW)	Equation
Lighting (P_{light})	$P_{light} = \begin{cases} P_l & \text{for night time travel} \\ 0 & \text{for day time travel} \end{cases}$
Air-conditioner - A/C (P_{AC})	$P_{AC} = \begin{cases} P_{cooling}(T_{cabin} - T_{req}) & \text{cooling} \\ P_{heating}(T_{req} - T_{cabin}) & \text{heating} \\ 0 & \text{OFF condition} \end{cases}$
Wipers (P_{wip})	$P_{wip} = P(rain)P_{wipers}$
Indicator ($P_{indicator}$)	$P_{indicator} = nP_{turn}$

The total power consumed by auxiliary loads can then be calculated as:

$$P_{aux} = P_{light} + P_{AC} + P_{wip} + P_{indicator} \quad (1)$$

3.3 Conclusion

The total power requirement in an EV when it is travelling along a user defined path was studied and the equations were derived.

CHAPTER 4

SoC ESTIMATION AND RANGE PREDICTION

4.1 Introduction

The selection of an appropriate battery model is very important for SoC estimation. With the help of battery model the dynamics of the battery could be understood and the prediction can be done with least error [18]. In this chapter firstly the battery model is taken, and its peculiarities and state space equations are derived. After this Extended Kalman Filter algorithm is applied to find the current SoC of the cell. Once the current SoC and the energy required for trip are calculated, the range of the EV can be predicted. The logical flow of EKF algorithm, battery pack SoC estimation, range prediction etc. are explained in detail in the coming sections.

4.2 Thevenin battery model

In this study lithium-ion cell was taken as it has high energy-density, less self-discharge rates and it is used in most of the EV's. The battery model selected was Thevenin 1st order RC battery model because the dynamics characteristics could be simulated easily. Figure 4.1 shows the Thevenin battery model of a lithium-ion cell [19].

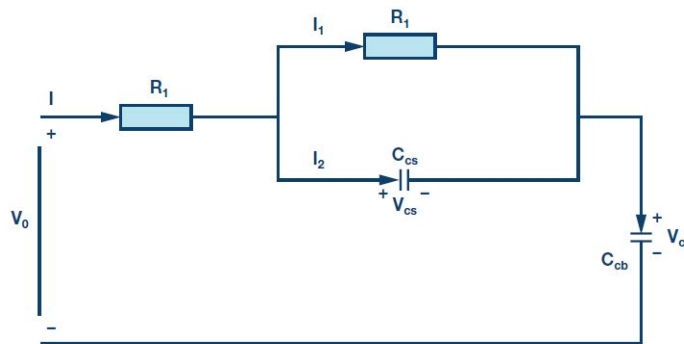


Figure 4.1: Thevenin battery model of a lithium-ion cell.

The parameters $V_{oc}, V_o, I, R_d, R_i, C_d, C_b$ are open circuit voltage, output voltage, charging or discharging current, polarization resistance, internal resistance, surface capacitance and bulk capacitance of the battery model respectively. From the battery model the below equations were obtained.

$$\dot{V}_{oc} = \frac{I}{C_b} \quad (2)$$

$$\dot{V}_d = \frac{I}{C_d} - \frac{V_d}{R_d C_d} \quad (3)$$

$$V_o = V_{oc} + V_d + IR_i \quad (4)$$

Open circuit voltage of a battery is a nonlinear function of state of charge. Hence this relation can be expressed as:

$$V_{oc} = aSoC + b \quad (5)$$

where the variables a and b are not constants and they vary with state of charge and temperature. Considering SoC and V_d as states, the state equation and the measurement equation can be obtained from the above battery model as shown below.

$$SoC = \frac{I}{aC_b} \quad (6)$$

$$\dot{V}_d = \frac{I}{C_d} - \frac{V_d}{R_d C_d} \quad (7)$$

4.3 Extended Kalman Filter algorithm

Kalman Filter is a linear state estimator. With the help of Kalman filter the error in estimating the states can be reduced greatly by the selection of appropriate error covariances. Kalman filter can be applied to linear systems only. For non-linear systems it can't be applied directly. So Taylor series expansion of the state and measurement equations are taken at the operating points and then Kalman Filter algorithm is applied. This is known as EKF algorithm as it is the extended version of

Kalman Filter. Other than EKF, algorithms like Adaptive Kalman Filter (AKF), Unscented Kalman Filter (UKF) and Particle Filter can be applied [20], [21]. Here in this study EKF was selected as the computations involved are less and the error in estimation is also negligible. Figure 4.2 gives a brief idea on the terms predicted state, optimal state estimate and measured state [22].

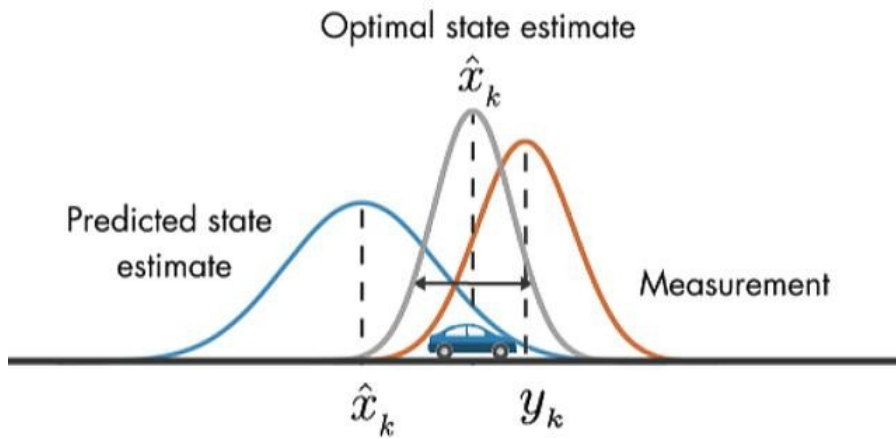


Figure 4.2: Terms related to state estimation.

The battery model can be expressed as:

$$\dot{x} = s(x, u) + q$$

$$y = m(x, u) + r$$

where $s(x, u)$ is the state equation, $m(x, u)$ is the measurement equation, y is the output matrix, x is the state matrix, q and r are process noise and measurement noise respectively. Then the below can be deduced as:

$$s(x, u) = \begin{bmatrix} \frac{I}{aC_b} \\ \frac{I}{C_d} - \frac{V_d}{R_d C_d} \end{bmatrix} \quad (8)$$

$$m(x, u) = aSoC + V_d + IR_i + b \quad (9)$$

The KF algorithm has two steps of computation namely prediction step and update step. In prediction step error covariance is predicted from the given values of process noise, measurement noise, and initial state. Once the predictions are made, Kalman gain is found and the states of the system and error covariance are updated which comes under update step. Figure 4.3 [23] shows the flow of KF algorithm. The state space representation of any system can be written as:

$$\dot{x} = A_m x + B_m u$$

$$y = C_m x + D_m u$$

Since discrete EKF is used, the battery model equations should be discretized after linearization. For linearizing the system, Taylor series expansion of the battery model equations are taken at the operating points. Let the states of the system be SoC (denoted as x_1), V_d (denoted as x_2) and the input be I (denoted as u). Then the equations (8) and (9) can be rewritten as:

$$s(x, u) = \begin{bmatrix} s_1 \\ s_2 \end{bmatrix} = \begin{bmatrix} \frac{u}{aC_b} \\ \frac{u}{C_d} - \frac{x_2}{R_d C_d} \end{bmatrix} \quad (10)$$

$$m(x, u) = ax_1 + x_2 + uR_i + b \quad (11)$$

The battery model after linearization can be written as:

$$\dot{x} = A_k x + B_k u$$

$$y = C_k x + D_k u$$

where

$$A_k = \begin{bmatrix} \frac{\partial s_1}{\partial x_1} & \frac{\partial s_1}{\partial x_2} \\ \frac{\partial s_2}{\partial x_1} & \frac{\partial s_2}{\partial x_2} \end{bmatrix} = \begin{bmatrix} 0 & 0 \\ 0 & \frac{-1}{R_d C_d} \end{bmatrix}, \quad B_k = \begin{bmatrix} \frac{\partial s_1}{\partial u} \\ \frac{\partial s_2}{\partial u} \end{bmatrix} = \begin{bmatrix} \frac{1}{aC_b} \\ \frac{1}{C_d} \end{bmatrix}$$

$$C_k = \begin{bmatrix} \frac{\partial m}{\partial x_1} & \frac{\partial m}{\partial x_2} \end{bmatrix} = \begin{bmatrix} a & 1 \end{bmatrix}, \quad D_k = \begin{bmatrix} \frac{\partial m}{\partial u} \end{bmatrix} = R_i$$

Now the battery model which is linearized is obtained. The linearized battery model can be discretized as shown below.

Consider the above model with the matrices A_k, B_k, C_k and D_k . Then the state equation can be written as:

$$\begin{aligned}\dot{x} &= A_k x + B_k u \\ \frac{x_{k+1} - x_k}{T_s} &= A_k x_k + B_k u_k \\ x_{k+1} - x_k &= A_k x_k T_s + B_k u_k T_s \\ x_{k+1} &= x_k + A_k x_k T_s + B_k u_k T_s \\ x_{k+1} &= (I + A_k T_s) x_k + B_k T_s u_k\end{aligned}$$

Let the term $(I + A_k T_s) = A$ and $B_k T_s = B$. Then state equation can be written as:

$$x_{k+1} = Ax_k + Bu_k$$

Similarly, the output equation can be written as:

$$y_{k+1} = Cx_k + Du_k, \text{ where } C = C_k \text{ and } D = D_k$$

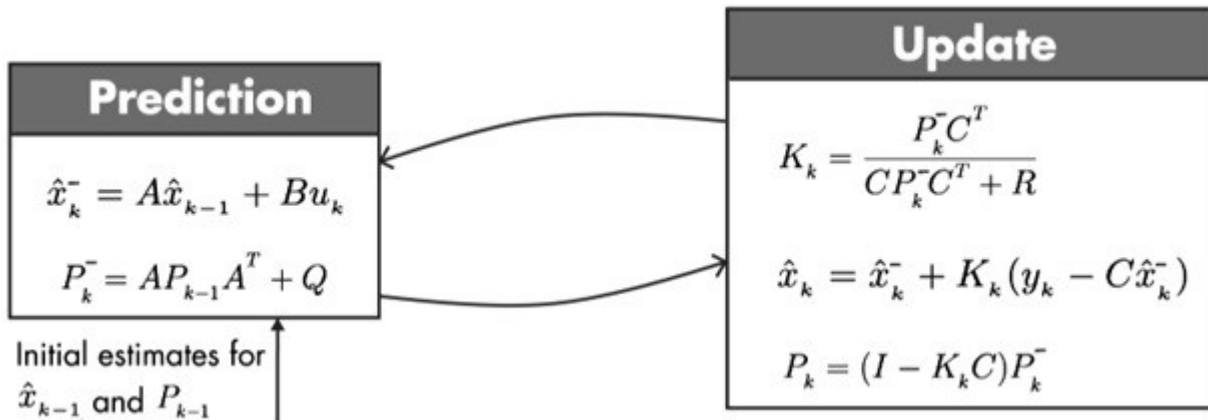


Figure 4.3: Kalman Filter algorithm.

The variables P_k , K_k , Q and R are error covariance, kalman gain, process noise covariance and measurement noise covariance respectively.

4.4 SoC estimation of the battery pack

SoC or state of charge is the percentage of total capacity available to power a load. In the previous sections, battery model and the state and measurement equations were derived which gives us an idea about the discharge and charging pattern of the battery. From the above sections the total power consumed from battery can be calculated as:

$$P_{batt} = P_{tra} + P_{inv} + P_{ind} + P_{aux} \quad (10)$$

If I_{batt} is the current drawn from battery and V_{batt} is the voltage of battery pack, then:

$$I_{batt} = \frac{P_{batt}}{V_{batt}} \quad (11)$$

Finally from the above two equation, we can write:

$$SoC_{final} = SoC_{init} - \frac{1}{capacity_{battery}} \sum_{k=1}^K I_{batt,k} t_k \quad (12)$$

where SoC_{init} , t_k and $I_{batt,k}$ are the initial value of SoC obtained from KF, time spent (hrs) in between k and k-1 segments and current consumed (amps) in each segment.

4.5 Range estimation

This section deals with the prediction of available driving range at any instant of a particular battery SoC value. The user will be asked to enter the source and destination points and the total power which will be consumed for traveling from source to destination will be calculated. Once the total energy or power prediction is made, the range available can also be predicted. While predicting the available driving range, three scenarios may arise. They are given in the below Figure 4.4.

Table 4.1: Driving scenarios.

Scenario	Drivable trip distance	Remaining range after trip
SoC becomes min. allowed value exactly at the destination	Distance between source and destination.	0kms
SoC becomes the min. allowed value at a location A between source and destination.	Distance between source and the location A.	0kms
SoC is more than the min. allowed value, at destination	Distance between source and destination.	History based range estimation

As said above, the user is asked to provide source and destination details. With the provided details the total power which will be consumed for the journey is calculated. The range is calculated until the SoC of the battery becomes the minimum allowed value.

The terms drivable trip distance denotes how much of the distance between the source and destination the EV can travel. In the first scenario, exactly at the destination SoC becomes min. allowed value. Then the drivable trip distance is the distance between source and destination. Since the SoC has reached the minimum allowed value, no more travelling is possible. Hence remaining range after the trip is zero. Consider a location A between source and destination as shown in the Figure 4.5.

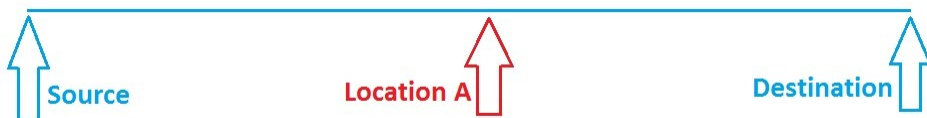


Figure 4.4: Representation of locations.

In the second scenario at location A, SoC becomes the minimum allowed value. Then the drivable trip distance is the distance between location A and source. Here also the remaining

range after the trip is zero, as the SoC has reached the minimum allowed value. In the third scenario, even after reaching the destination the SoC is greater than the minimum allowed value. So there is some more SoC left that can be used for travelling. If the user is not selecting one more destination the remaining range can't be told directly as the next destination point is unknown for the system. Moreover the climate conditions, road grade or elevation details etc. won't be available and hence power consumption calculations can't be made. A history based range estimation is used in this scenario. The average energy consumption will be known to the system and using that the approximate range can be predicted. The remaining range available can be expressed as:

$$\text{Remaining range} = 100 \text{ km} \frac{E - \Delta E}{AEC} \quad (13)$$

where E and ΔE are energy available in battery and the energy consumed between destination and current locations.

4.6 Conclusion

In this chapter the reasons for selecting Li-ion battery and considering thevenin equivalent model were discussed. The state and measurement equations of the above battery model were derived and the importance of using Kalman filter was identified. The terms related to the filter and the algorithm flow were also discussed. The equation for final SoC with respect to current drawn from battery, initial SoC, battery capacity and time taken while charging/discharging was derived. The net change in SoC is found to be proportional to the power consumed.

In range prediction section the three scenarios which may arise while range prediction were identified. For each scenarios the different steps to find the drivable trip distance and remaining range after trip were calculated. The average energy consumption may be recorded and updated after every interval so that the calculations can be made more specific and the range prediction can be made more accurate.

CHAPTER 5

SIMULATION AND EXPERIMENTAL RESULTS

Before moving to simulation and experimental results the overview of the system selected for the study should be explained, which is done in the below section.

5.1 System Overview

This section deals with explaining the overview of the system selected for study. The block diagram of range estimation block, the specifications of the system, EV parameters etc. are discussed here.

5.1.1 Range estimation block

The Figure 5.1 shown below corresponds to the simulink block of range estimation. Once user enters his source and destination location, the value of current SoC is taken from EKF block and the energy required for traveling from source point to destination is calculated. Once the enrgy required for trip is obtained, the decisions on remaining range can be done.

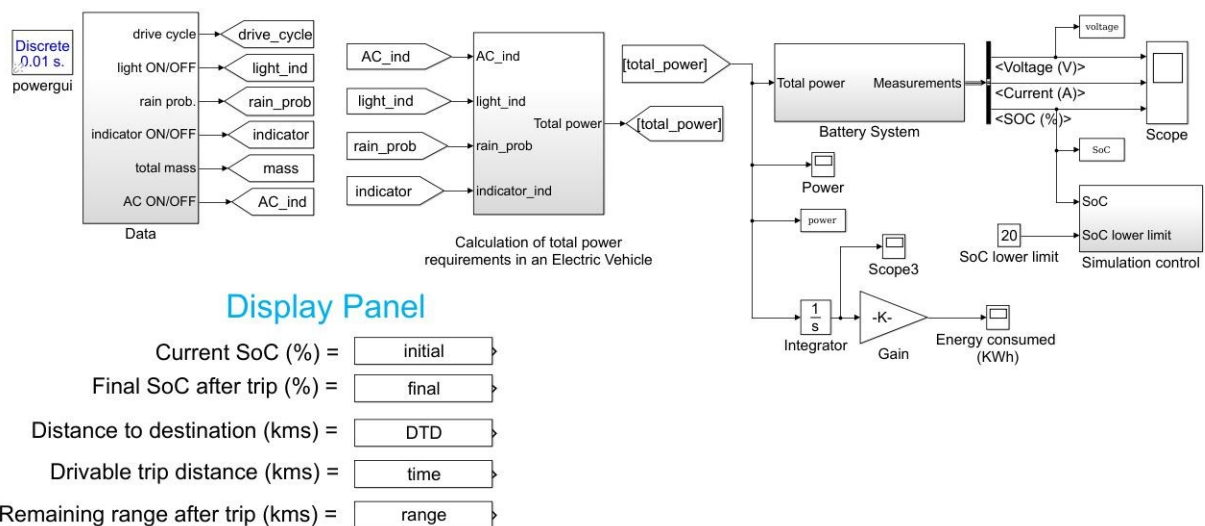


Figure 5.1: Range estimation block.

This simulation block consists of the below four main subsystems.

- Data subsystem – This subsystem block consists of all the data, declared variables, constants etc. required to run the simulation. The data includes mass of the vehicle, drive cycle from range estimation block, probability of rain, auxiliary load usage, elevation of the road etc.
- Power requirement calculation subsystem – The data from data subsystem is fed into this block and it's here the total power requirement in travelling from user defined source to destination is calculated. The output of this block is total power consumption over time.
- Battery system – This block mainly consists of EV battery and the battery charging/discharging circuit. The input to this block is the total power consumption and the outputs are the voltage, current, SoC measurements. From total power requirement, the instantaneous current that should be drawn from the battery is calculated. The variation in voltage, current and SoC can be noticed through scopes at the output.
- Simulation control subsystem – This subsystem decides how much time the simulation has to run, where the key parameter which decides this is the SoC lower limit. SoC lower limit defines the minimum value of SoC up to which the battery can be drained or discharged. After this current can't be taken from battery. So the battery needs to be recharged for further use. In this study the value of SoC lower limit is taken as 20.

There is a display panel which shows the details such as Current SoC, Final SoC after the trip, Distance to destination, Drivable trip distance (how much of the distance between source and destination can the EV travel with the available SoC at that time) and Remaining range after the

trip. Initially the values are not displayed. Once the simulation starts and the simulation control system stops the simulation the values are populated in the display panel.

5.1.2 EV parameters and system specifications

The EV parameters and system specifications are the values assigned to the variables of the system and EV for running the simulation. The assigned values are given in the Table 5.1 shown below.

Table 5.1: EV parameters and system specifications.

Parameter	Symbol	Value
Total mass of the EV	m	1558kg
Acceleration due to gravity	g	9.8 m/sec ²
Density of air	ρ_{air}	1.225 kg/m ³
Frontal area	A_f	2.5 m ²
Drag coefficient	C_d	0.3
Battery nominal voltage	V	400V
Battery capacity	Ah	60Ah
SoC lower limit	Ah	20% of total battery capacity

The simulation was carried out with the above mentioned values of system parameters. In the next section the simulink model of EKF based SoC estimation, range predictor model and the results obtained are explained.

5.2 Simulation Results

As a part of study, the simulink model of EKF based SoC estimation and range predictor model were designed. The findings and results obtained are discussed here in this section. The simulink model of EKF based SoC estimation of a lithium-ion cell is shown in Figure 5.2. Here a lithium-ion cell (4V, 30Ah) at 100% SoC is taken and discharged non-uniformly using a current pulse

generator till 5%. The current flowing through the cell and the voltage across the cell terminals are given to the state equation block and measurement equation block after adding random noise of known co-variance. Hence 2 sets of values are obtained: the true value - which is the actual value and the measured value - which consists of noise. The measured value 'y' is then given to Extended Kalman Filter block and the value of SoC is obtained at the output.

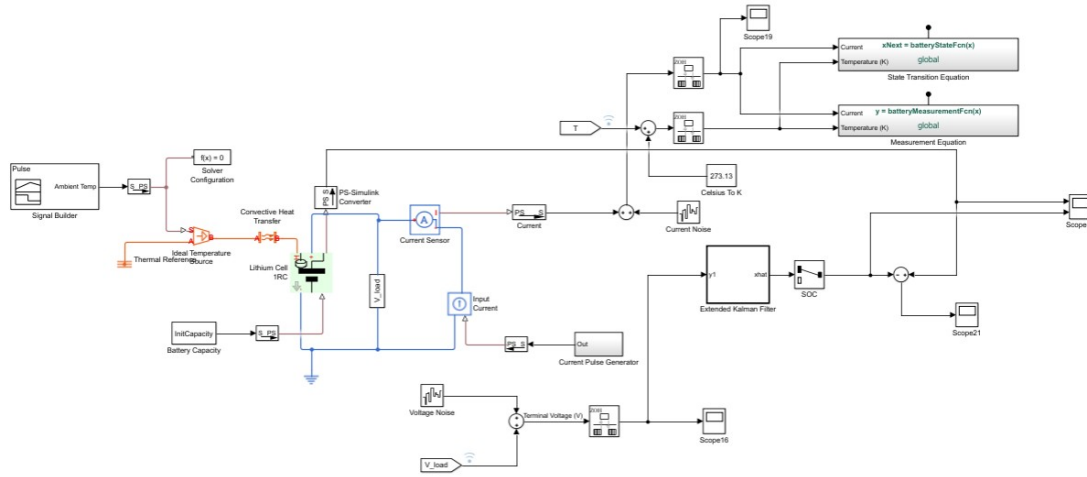


Figure 5.2: SoC estimation of Lithium-Ion cell using EKF.

The actual SoC of the cell is obtained from the lithium-ion cell model and the estimated SoC is obtained from output of the EKF block. When compared it was found that the estimated value following the actual value with a maximum error of 0.01. Real SoC vs estimated SoC, error in estimation are displayed in the figures 5.3 and 5.4.

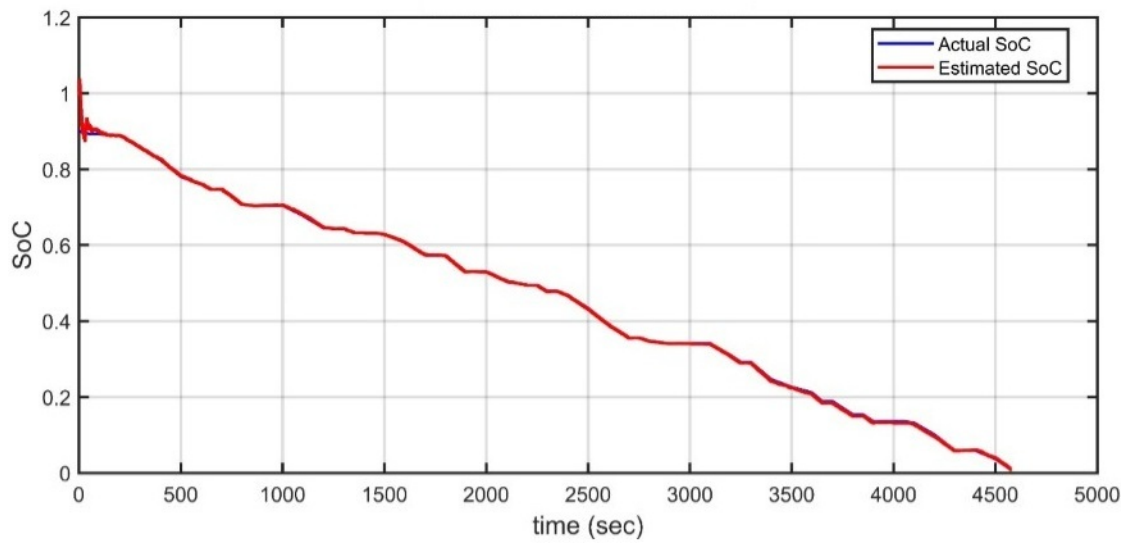


Figure 5.3: Actual SoC vs Estimated SoC.

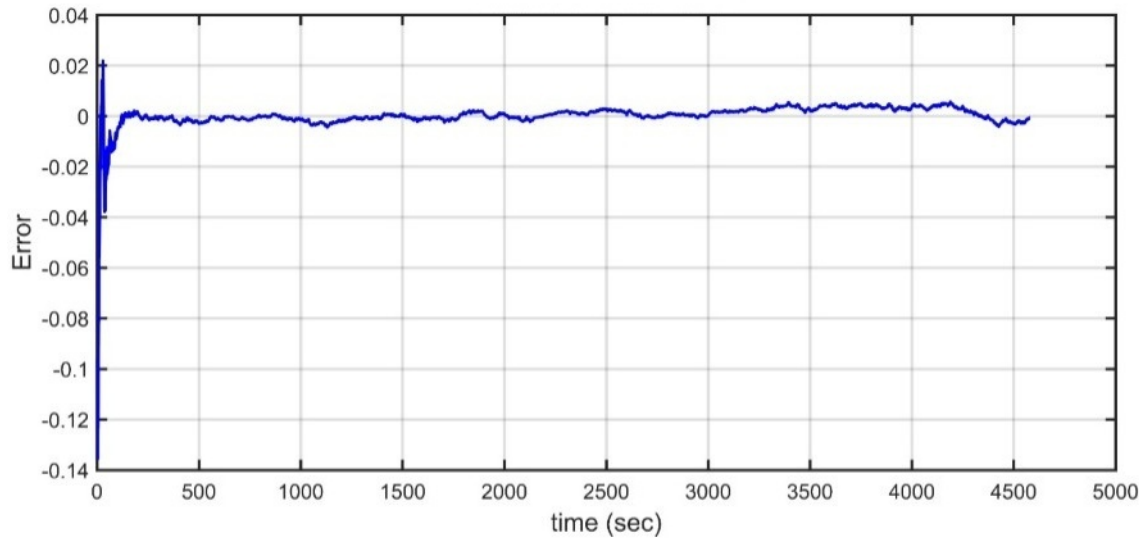


Figure 5.4: Error in SoC estimation.

The values of process noise covariance (Q), measurement noise covariance (R), error covariance (P) and initial state (x) needs to be given to the EKF block for estimation. Below are the values which were provided as initial inputs:

$$x = \begin{bmatrix} 1 \\ 0 \end{bmatrix}, \quad P = \begin{bmatrix} 0.01 & 0 \\ 0 & 1 \end{bmatrix}, \quad Q = \begin{bmatrix} 2e-8 & 0 \\ 0 & 3e-7 \end{bmatrix} \quad \text{and} \quad R = \begin{bmatrix} 1e-3 \end{bmatrix}$$

Here the current pulse used for discharging cell is also the current flowing through battery. The voltage across terminals of the cell and the current flowing through the battery is shown in figures 5.5 and 5.6.

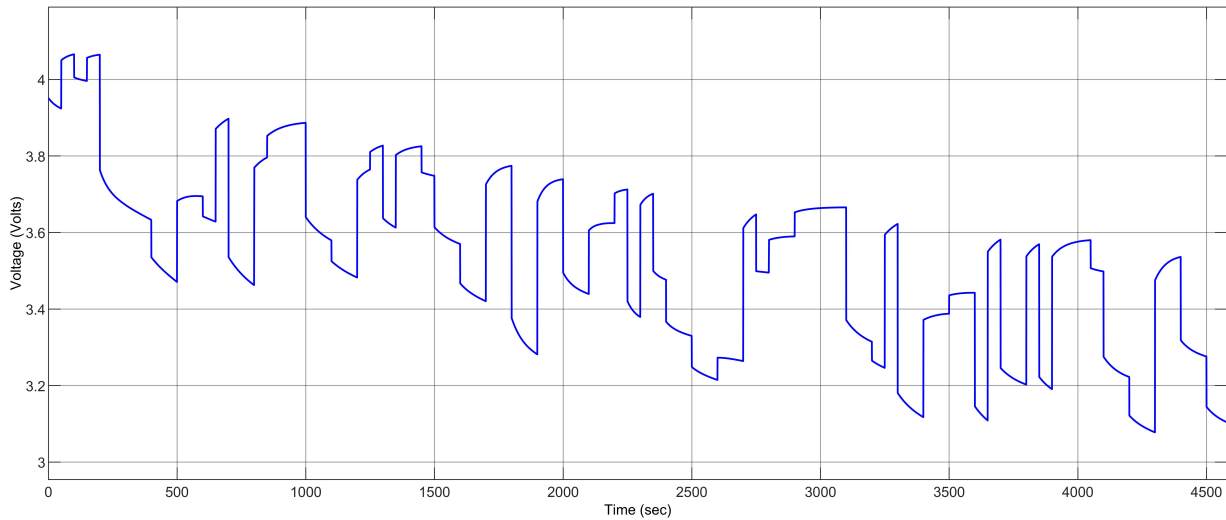


Figure 5.5: Variation of voltage with SoC.

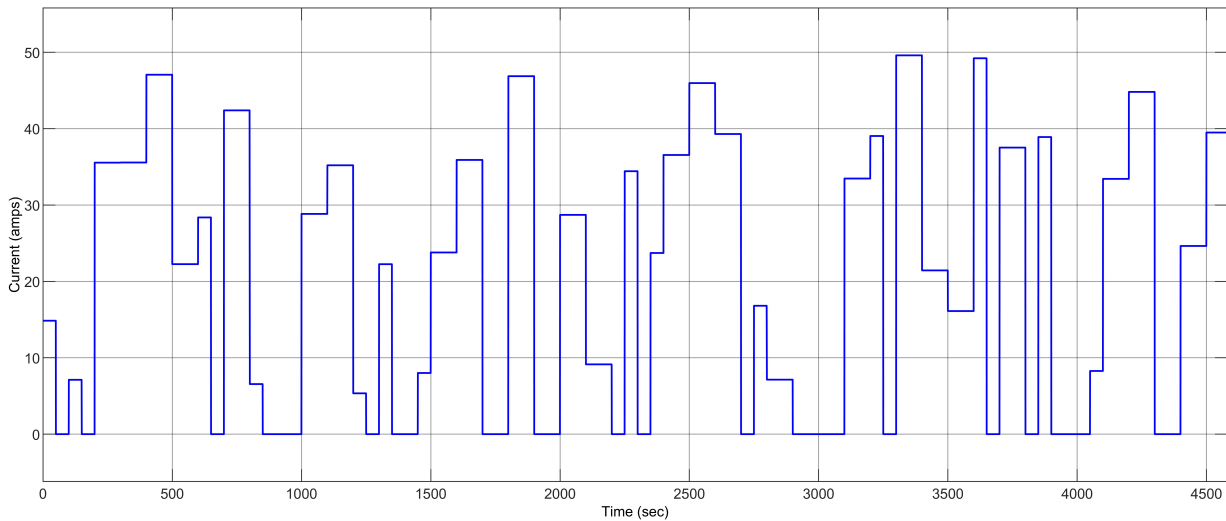


Figure 5.6: Current flowing through battery.

Once SoC estimation is done, the value of current SoC is fed to the range predictor block. As mentioned above three driving scenarios exist. The model was simulated for these three scenarios and results were obtained. The driving range available in three scenarios are discussed in detail below. The three scenarios are explained assuming that the driver or user has selected the source and destination points. Let A be a location in between source and destination as mentioned in the chapter - SoC estimation and range prediction.

5.2.1 Driving Scenario - 1

In the first driving scenario the range predictor model simulates and finds that the SoC becomes minimum allowed value (SoC lower limit) exactly at the destination. i.e. there is no more enough charge available in the battery to drive the vehicle. Hence the drivable trip is the distance between source and destination and the remaining range after the user defined trip is zero. These details are populated appropriately in the display panel of the range predictor model. The simulation results obtained for this scenario is given in Figure 5.7.

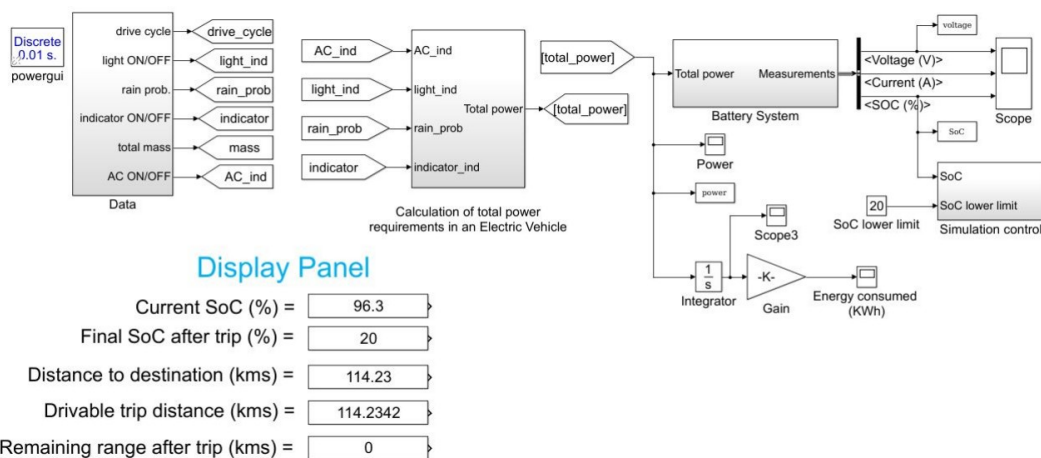


Figure 5.7: Simulation results of driving scenario - 1

5.2.2 Driving Scenario - 2

In the second driving scenario the range predictor model simulates and finds that the SoC becomes the minimum allowed value (SoC lower limit) at a location A between source and destination. i.e.

there is no enough charge available in the battery to drive the vehicle till destination. There is only charge available to reach till the location A. Hence the drivable trip is the distance between source and the location A and the remaining range after the user defined trip is zero. These details are populated appropriately in the display panel of the range predictor model. The simulation results obtained for this scenario is given in Figure 5.8.

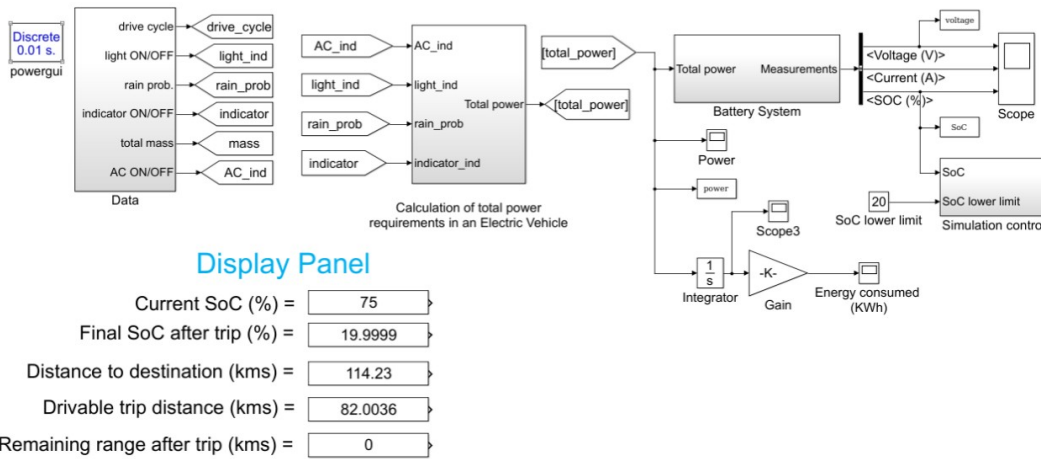


Figure 5.8: Simulation results of driving scenario - 2.

5.2.3 Driving Scenario - 3

In the third driving scenario the range predictor model simulates and finds that the SoC is more than the minimum allowed value at destination. i.e. there is charge available in the battery to drive the vehicle even after destination. Hence the drivable trip is the distance between source and the location A. As there is charge more than SoC lower limit available in the battery, the remaining range after the user defined trip is not zero. If the user is not inputting another destination location the elevation details of the road, climatic conditions etc. are unknown to the system. In that case a history based range estimation is employed. Here the average energy consumption (AEC) of the vehicle is used to calculate the remaining range available after the trip. The AEC keeps on updating whenever the EV is travelling. From this the performance of the EV can also be estimated. The details like drivable range, remaining range, distance to destination etc. are populated appropriately in the display panel of the range predictor model. The simulation results obtained for this scenario

is given in Figure 5.9.

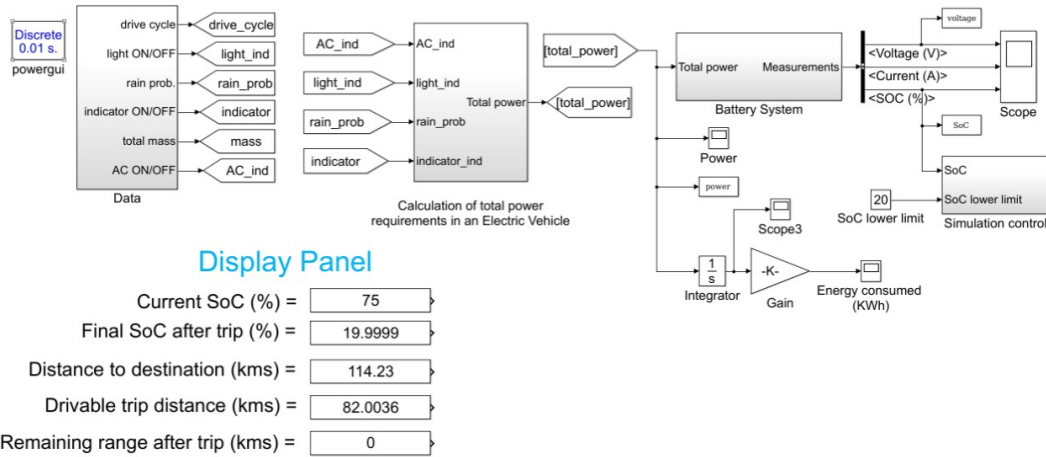


Figure 5.9: Simulation results of driving scenario - 3.

The obtained results were compared with the true data available and it was found that the simulated power, estimated driving range, estimated remaining range etc. are on par with the true values. The true data values were obtained from a website named Charge Car. The drive information, trip statistics etc. of a particular trip was taken and these details were given to the range predictor model. Once simulated it was found that the estimated values given by the model were almost equal to the true values mentioned in the website. The drive information and trip statistics are given in Figure 5.10 [24].

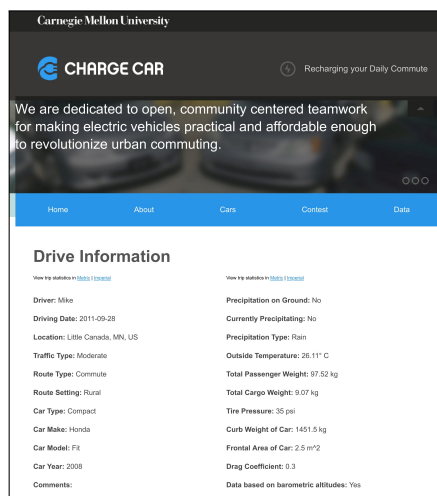


Figure 5.10: Electric car trip statistics and drive information

As the vehicle is traveling, energy is taken from the battery to meet the power requirements for traveling from source to destination. The total power consumption largely depends on the drive cycle which the EV follows. Here the drive cycle EV has followed is shown in Figure 5.11.

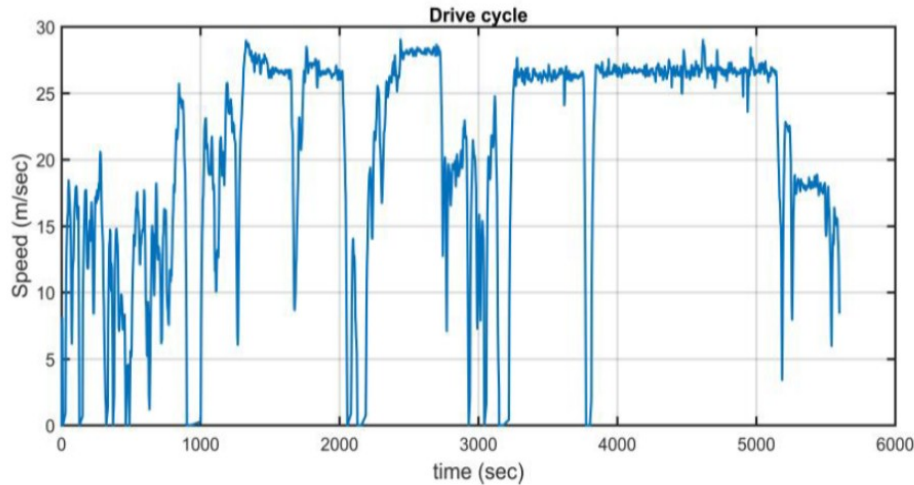


Figure 5.11: Drive cycle vs Journey time.

As SoC varies from 100% to SoC lower limit (20%) the voltage of the battery also reduces. The variation of voltage, current, SoC and energy consumption with respect to journey time is shown in the figures 5.12, 5.13, 5.14 and 5.15 respectively.

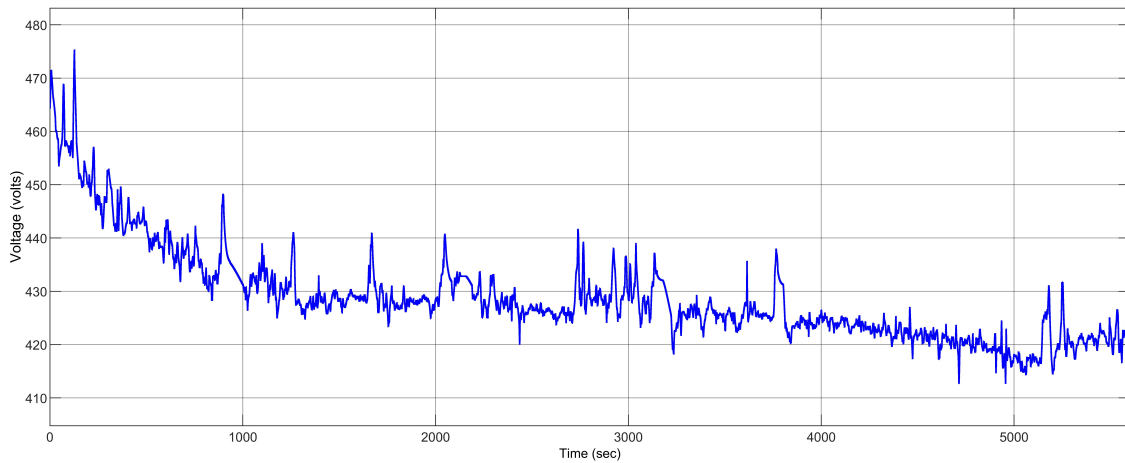


Figure 5.12: Battery voltage vs Journey time.

The battery voltage was found to be varying in between 470V and 415V when the battery pack was discharged from 100% to almost 20%.

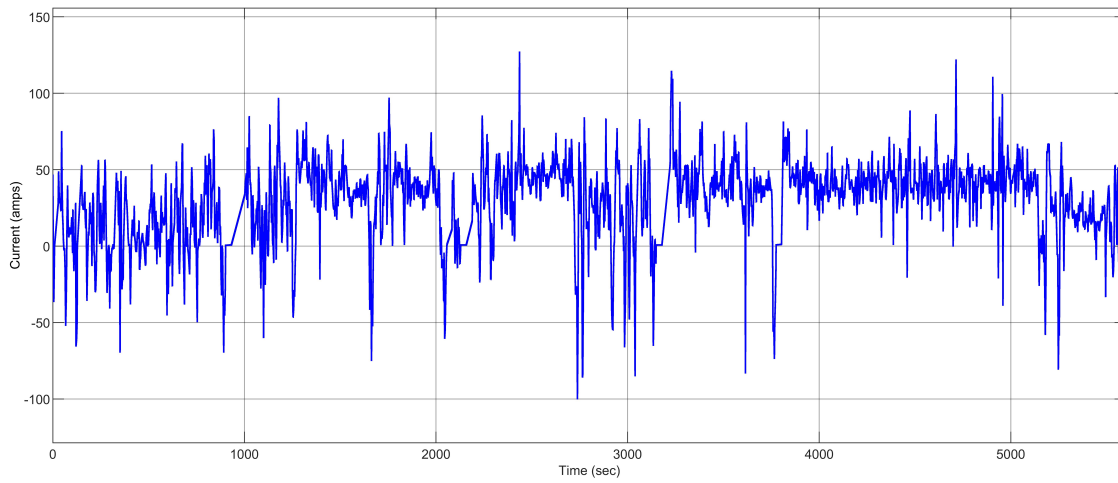


Figure 5.13: Battery current vs Journey time.

The current waveform is shown to be taking positive and negative values. When current is positive, the battery is being discharged and power is being fed to drive the vehicle. When the current becomes negative, regeneration action takes place and the battery gets charged.

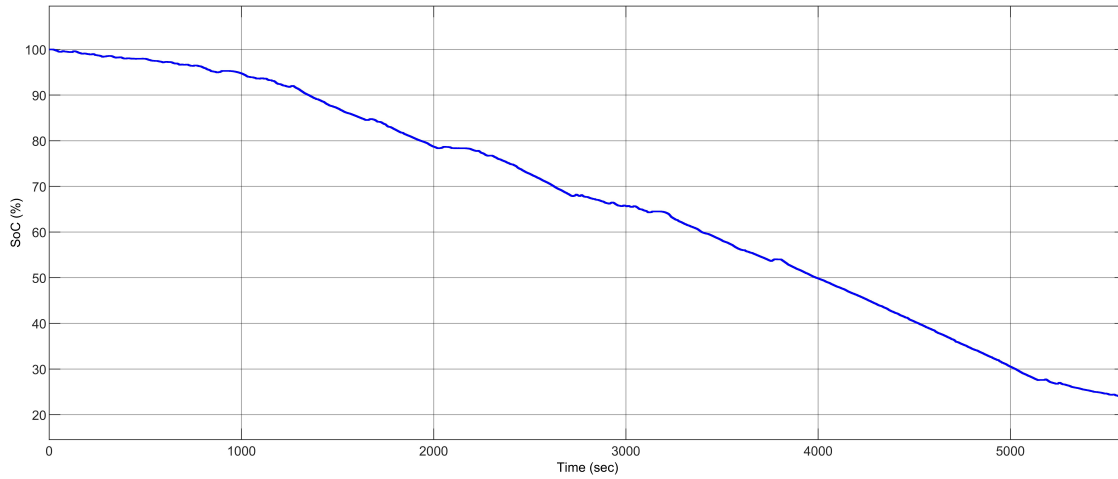


Figure 5.14: Battery SoC vs Journey time.

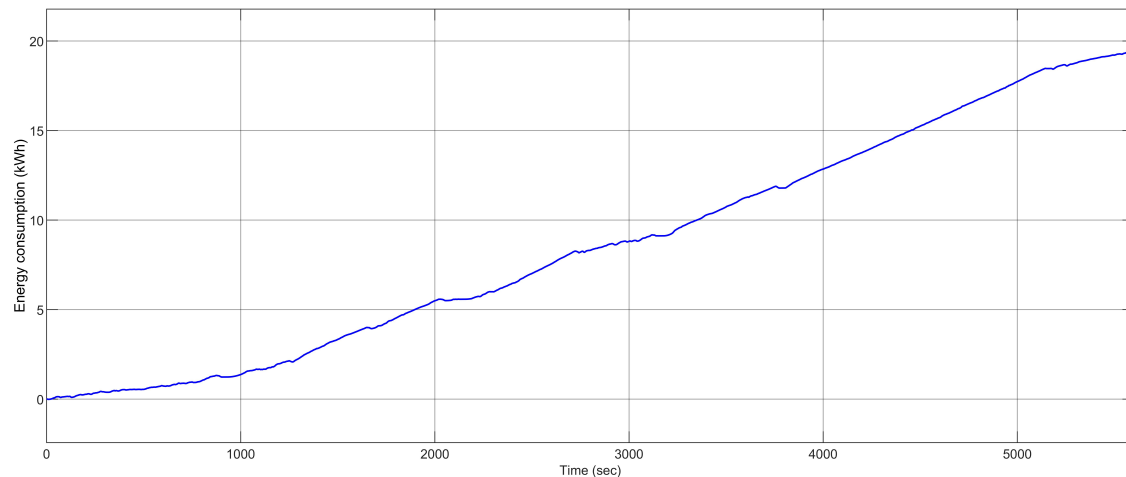


Figure 5.15: Energy consumption vs Journey time.

The estimated total power consumption aligns with the true power consumption. The Figure 5.16 shown below shows the real time and the simulated power.

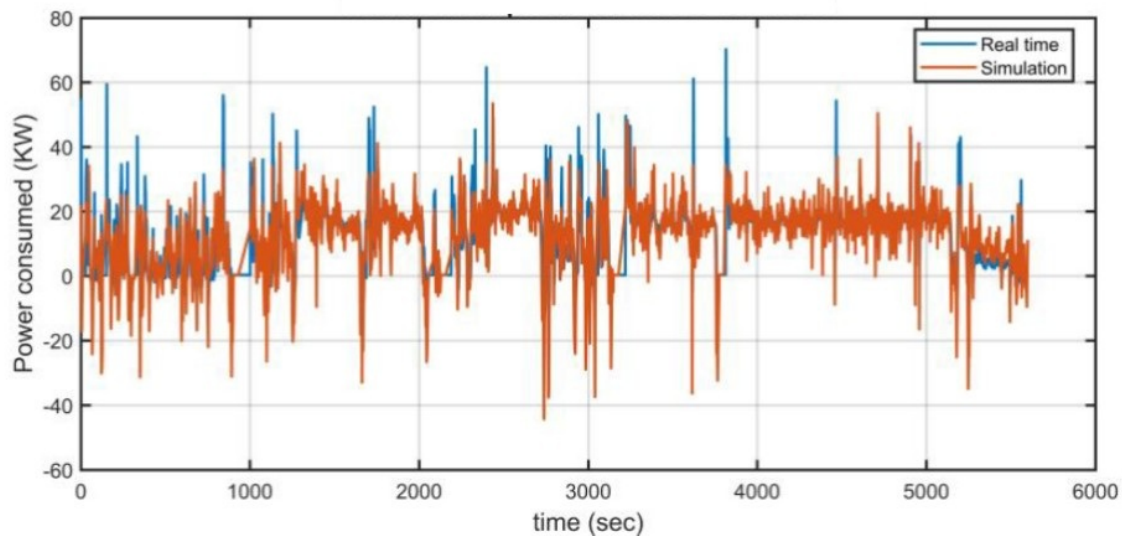


Figure 5.16: Real time power vs Simulated power

5.3 Hardware results

Once the simulation was done and it was found to be working fine, hardware for battery SoC using EKF was implemented. The Figure 5.17 and 5.18 shows the implemented hardware setup and the voltage & current sensor used.



Figure 5.17: Hardware setup.

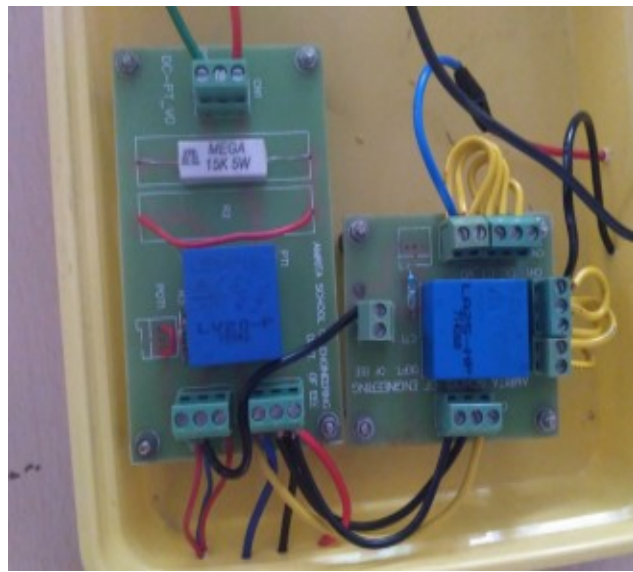


Figure 5.18: Voltage transducer and Current transducer.

The components used are given below:

- 12V, 7Ah battery
- 60W, 48V, 1.2A, 1500 rpm - DC motor
- LA 25-NP current transducer, $5\text{k}\Omega$ resistor
- LV 20-P voltage transducer, $15\text{k}\Omega$ 5W power resistor and $2\text{k}\Omega$ resistor
- 43Ω , 2.8A rheostat
- Voltage supply: +15V -15V and COM
- Raspberry Pi 3 Model B+
- Arduino Uno
- DPST switch - act as ignition switch

The battery was connected in series to a variable rheostat and DC motor. Once the DPST switch is closed the circuit becomes closed and current is drawn from the battery to drive the DC motor. At different positions of the rheostat the net voltage across the DC motor terminals gets varied and thus the speed of the motor also varies. Hence it can be said that the DC motor is following a particular drive cycle, rather than running at constant speed. Since there is speed variation the current drawn is also nonuniform. Here arduino was used for serial communication with raspberry pi. Since raspberry pi doesn't have any analog pins the voltage and current values can't be measured directly and given to the algorithm. Since both current and voltage measurements are required, two ADC's are required. A 10 bit ADC output will be available at 10 pins. i.e. for measuring two analog values using two 10 bit ADC's 20 pins are required which makes the circuit bulky and the code complex. To keep the work simple yet very effective an arduino uno was used to measure analog value as well as to communicate with the raspberry pi. The analog readings will be read by arduino uno which has 10 bit internal ADC and this is given to raspberry pi via serial communication. Once

the data is received, these values are taken and passed to the EKF algorithm for SoC prediction. The implemented hardware system was found to be able to estimate SoC with good precision and accuracy.

Below given are the list of software tools used:

- Thonny Python IDE
- Arduino IDE
- MATLAB Simulink

The voltage sensor (PT) and current sensor(CT) used are LV 20-P and LA 25-NP. The design of PT and CT is given below.

5.3.1 Design of PT

The model of PT selected was LV 20-P. It is a closed loop compensated voltage transducer that works under the principle of hall effect. Since the battery used is 12V, 7AH - the max voltage that may be applied across the PT was assumed to be 15V. In the primary of PT only current less than 10mA should be allowed.

The conversion ratio of the PT is 2500 : 1000.

$$\text{Assume } I_1 = 1\text{mA, then resistance to be connected on primary- } R_1 = \frac{V_{max}}{I_1} = \frac{15V}{1mA} = 15k\Omega$$

$$\text{As per conversion ratio, } \frac{I_2}{I_1} = \frac{N_1}{N_2} = \frac{2500}{1000} = 2.5$$

$$\text{i.e. } I_2 = 2.5I_1 = 2.5 \times 1\text{mA} = 2.5\text{mA}$$

For a voltage of 15 V applied at primary, a voltage of 5V is expected at the output.

Then $I_1 = 1\text{mA}$, $I_2 = 2.5 \text{ mA}$ and $R_o = \frac{5}{2.5mA} = 2k\Omega$, where R_o is the resistance to be connected on secondary across which the measurement is taken. From the above design procedure the value of R_i and R_o was obtained as $15k\Omega$ and $2k\Omega$ respectively. Figure 5.19 [25] shows the image of a LV 20-P voltage transducer.



Figure 5.19: Voltage transducer LV 20-P.

Conversion factor: Input voltage applied = $3 \times$ voltage measured across R_o

5.3.2 Design of CT

The model of CT selected was LA 25-NP. It is a closed loop compensated current transducer that works under the principle of hall effect.

The conversion ratio of the CT is 1:1000.

$$\text{i.e. } \frac{I_2}{I_1} = \frac{N_1}{N_2} = \frac{1}{1000} = 0.001 \text{ or } I_2 = I_1 \times 10^{-3}$$

When a current of 1A flows in primary, a voltage of 5V is expected at the output.

So, when $I_1 = 1\text{A}$, then $I_2 = 1 \times 10^{-3} = 1\text{mA}$

i.e. the resistance to be connected on secondary across which the measurement is taken,

$$R_o = \frac{5}{1 \times 10^{-3}} = 5k\Omega$$

From the above design procedure the value of R_o was obtained as $5k\Omega$. Figure 5.20 [26] shows the image of a LA 25-NP current transducer.



Figure 5.20: Current transducer LA 25-NP.

Conversion factor: Input current = $0.2 \times$ voltage measured across R_o

With the help of PT and CT the battery voltage and current flowing through battery can be measured and send to raspberry pi via arduino for EKF based SoC estimation.

5.4 Conclusion

The simulink block of EKF based SoC estimation of a lithium-ion cell and range predictor model was developed in MATLAB 2018a. The EKF model was able to estimate SoC with a maximum error of 0.01 and the range predictor model gave output matching the true values of power consumption and remaining driving range. A hardware setup was implemented that could measure the SoC of the battery, with the help of sensors PT and CT. The design of PT and CT were done to find the values of input resistance, output resistance or measuring resistance. The implemented system was found to be estimating SoC with good precision and accuracy.

CHAPTER 6

CONCLUSION AND FUTURE SCOPE

In this study two simulink models namely range predictor model and SoC estimation model were built. The range predictor model was able to simulate total power consumption, variation in battery voltage, variation in battery current, variation in battery SoC and predict the SoC after the trip, drivable range, remaining range after trip with high level of precision and accuracy. These obtained values were matching with real time results. The SoC estimation model was able to predict SoC with a maximum error of 0.01. The range predictor model considered all the power requirements while traveling from source to destination. If the system gets an idea about EV's current location, the nearby charging stations and the charger details can be displayed. For each charging station the power rating of chargers may vary depending on the number of charging slots, grid power availability etc. If the charger rating is also known to the system, the time required for charging to a particular SoC limit can also be found out.

REFERENCES

- [1] V. R. Tannahill, K. M. Muttaqi, and D. Sutanto, “Driver alerting system using range estimation of electric vehicles in real time under dynamically varying environmental conditions,” *IET Electr. Syst. Transp.*, vol. 6, no. 2, pp. 107–116, 2016.
- [2] “Elevation Service.” [Online]. Available: <https://developers.google.com/maps/documentation/javascript/elevation>.
- [3] A. Wolf, “Map-Based Driving Cycle Generation,” Electrotechnical Institute (ETI), 2015.
- [4] C. De Cauwer, W. Verbeke, T. Coosemans, S. Faid, and J. Van Mierlo, “A data-driven method for energy consumption prediction and energy-efficient routing of electric vehicles in real-world conditions,” *Energies*, vol. 10, no. 5, 2017.
- [5] Arunkumar P and VijithK, “IOT Enabled smart charging stations for Electric Vehicle,” *Int. J. Pure Appl. Math.* , vol. 119, no. 7, pp. 247–252, 2018.
- [6] “A more accurate way of predicting your range.” [Online]. Available: <https://jpwhitetesla.com/2012/04/12/a-more-accurate-way-of-predicting-your-range/>.
- [7] “2018 Nissan Leaf battery real specs.” [Online]. Available: <https://pushevs.com/2018/01/29/2018-nissan-leaf-battery-real-specs/>.
- [8] T. Williams, “Range.” [Online]. Available: <http://www.mynissanleaf.com/viewtopic.php?p=101293>.
- [9] “Model S: Driving Dynamics.” [Online]. Available: <https://teslamotorsclub.com/tmc/threads/wind-elevation-aware-range-prediction.40790/#post-870030>.
- [10] “Model S: User Interface.” [Online]. Available: <https://teslamotorsclub.com/tmc/threads/firmware-6-1.40577/page-2>.

- [11] “Evaluation and Observations with v6.1 Trip Energy Prediction.” [Online]. Available: <https://teslamotorsclub.com/tmc/threads/evaluation-and-observations-with-v6-1-trip-energy-prediction.41158/#post-877766>.
- [12] D. George, “TeslaFlux.” [Online]. Available: <http://www.teslaflux.com/>.
- [13] “2013 Tesla Model S Overview.” [Online]. Available: <https://www.hybridcars.com/2013-tesla-model-s-overview/>.
- [14] K. Sarrafan, D. Sutanto, K. M. Muttaqi, and G. Town, “Accurate range estimation for an electric vehicle including changing environmental conditions and traction system efficiency,” *IET Electrical Systems in Transportation*, 2017.
- [15] A. Enthaler and F. Gauterin, “Method for reducing uncertainties of predictive range estimation algorithms in electric vehicles,” *2015 IEEE 82nd Veh. Technol. Conf. VTC Fall 2015 - Proc.*, 2016.
- [16] Cedric De Cauwer, Joeri Van Mierlo and Thierry Coosemans, “Energy Consumption Prediction for Electric Vehicles Based on Real-World Data”, *Energies* 2015, 8, 8573-8593.
- [17] J. Hong, S. Park, and N. Chang, “Accurate remaining range estimation for Electric vehicles,” *Proc. Asia South Pacific Des. Autom. Conf. ASP-DAC*, vol. 25-28-Janu, pp. 781–786, 2016.
- [18] Zhihao Yu, Ruituo Huai and Linjing Xiao, “State-of-Charge Estimation for Lithium-Ion Batteries using a Kalman Filter Based on Local Linearization”, *Energies* 2015, 8, 7854-7873.
- [19] M. Murnane and A. Ghazel, “A Closer Look at State of Charge (SOC) and State of Health (SOH) Estimation Techniques for Batteries,” *Analog Devices*, 2017.
- [20] Z. Zeng, J. Tian, D. Li, and Y. Tian, “An online state of charge estimation algorithm for lithium-ion batteries using an improved adaptive Cubature Kalman filter,” *Energies*, vol. 11, no. 1, 2018.

- [21] R. Ramprasath and R. Shanmughasundaram, “STCKF Algorithm Based SOC Estimation of Li-Ion Battery by Dynamic Parameter,” *Advances in Signal Processing and Communication*, 2019, vol. 526, pp. 229–239.
- [22] “Understanding Kalman Filters, Part 3: An Optimal State Estimator.” [Online]. Available: <https://in.mathworks.com/videos/understanding-kalman-filters-part-3-optimal-state-estimator-1490710645421.html>.
- [23] “Extended Kalman Filter.” [Online]. Available: <https://balzer82.github.io/Kalman/>.
- [24] CREATE Lab - Carnegie Mellon University Robotics, “ChargeCar - Recharging your Daily Commute.” [Online]. Available: http://chargecar.org/meta_datas/738.
- [25] LEM, “Voltage Transducer LV 20-P.” [Online]. Available: https://media.digikey.com/pdf/data_sheets/lem_usa_pdfs/lv_20-p.pdf.
- [26] LEM, “LA 25-NP.” [Online]. Available: https://www.lem.com/sites/default/files/products_datasheets/la_25-np_sp7.pdf.
- [27] VISION, “Battery datasheet - CP1270.” [Online]. Available: <https://valbis.com/wp-content/uploads/2016/01/CP1270.pdf>.
- [28] “Raspberry Pi Compute Module 3+.” [Online]. Available: https://www.raspberrypi.org/documentation/hardware/computemodule/datasheets/rpi_DATA_CM3plus_1p0.pdf.

PUBLICATIONS

1. Pai. Sravan and M.R. Sindhu, "Intelligent driving range predictor for green transport," in *First International Conference on Materials Science and Manufacturing Technology (ICMSMT)*, 2019, vol. 3, no. April 2019, pp. 883–892.

APPENDIX A

LEM

Voltage Transducer LV 20-P

For the electronic measurement of voltages : DC, AC, pulsed..., with a galvanic isolation between the primary circuit (high voltage) and the secondary circuit (electronic circuit).



Electrical data

I_{PN}	Primary nominal r.m.s. current	10	mA
I_p	Primary current, measuring range	0 .. ± 14	mA
R_M	Measuring resistance	$R_{M\ min}$	$R_{M\ max}$
	with ± 12 V	@ ± 10 mA _{max}	30 190 Ω
		@ ± 14 mA _{max}	30 100 Ω
	with ± 15 V	@ ± 10 mA _{max}	100 350 Ω
		@ ± 14 mA _{max}	100 190 Ω
I_{SN}	Secondary nominal r.m.s. current	25	mA
K_N	Conversion ratio	2500 : 1000	
V_c	Supply voltage (± 5 %)	± 12 .. 15	V
I_c	Current consumption	10 (@±15V)+ I_s	mA
V_d	R.m.s. voltage for AC isolation test ¹⁾ , 50 Hz, 1 mn	2.5	kV

Accuracy - Dynamic performance data

X_G	Overall Accuracy @ I_{PN} , $T_A = 25^\circ C$	@ ± 12 .. 15 V	± 1.1	%
<input checked="" type="checkbox"/>	Linearity	@ ± 15 V (± 5 %)	± 1.0	%
			< 0.2	%
I_o	Offset current @ $I_p = 0$, $T_A = 25^\circ C$		Typ	Max
I_{OT}	Thermal drift of I_o	0°C .. + 25°C	± 0.20	mA
		+ 25°C .. + 70°C	± 0.10	± 0.30 mA
t_r	Response time ²⁾ @ 90 % of $V_{p\ max}$	40	μs	± 0.14 ± 0.40 mA

General data

T_A	Ambient operating temperature	0 .. + 70	°C
T_S	Ambient storage temperature	- 25 .. + 85	°C
R_p	Primary coil resistance @ $T_A = 70^\circ C$	250	Ω
R_s	Secondary coil resistance @ $T_A = 70^\circ C$	110	Ω
m	Mass	22	g
	Standards ³⁾	EN 50178	

Notes : 1) Between primary and secondary

2) $R_s = 25 \text{ k}\Omega$ (L/R constant, produced by the resistance and inductance of the primary circuit)

3) A list of corresponding tests is available

010802/0

$$I_{PN} = 10 \text{ mA}$$

$$V_{PN} = 10 .. 500 \text{ V}$$



Features

- Closed loop (compensated) voltage transducer using the Hall effect
- Insulated plastic case recognized according to UL 94-V0
- Optimized.

Principle of use

- For voltage measurements, a current proportional to the measured voltage must be passed through an external resistor R , which is selected by the user and installed in series with the primary circuit of the transducer.

Advantages

- Excellent accuracy
- Very good linearity
- Low thermal drift
- Low response time
- High bandwidth
- High immunity to external interference
- Low disturbance in common mode.

Applications

- AC variable speed drives and servo motor drives
- Static converters for DC motor drives
- Battery supplied applications
- Uninterruptible Power Supplies (UPS)
- Power supplies for welding applications.



Current Transducer LA 25-NP

$I_{PN} = 5-6-8-12-25 \text{ At}$

For the electronic measurement of currents: DC, AC, pulsed..., with galvanic isolation between the primary circuit and the secondary circuit.



16080



Electrical data

I_{PN}	Primary nominal current rms	25	At
I_{PM}	Primary current, measuring range	0 .. ± 36	At
R_M	Measuring resistance @	$T_A = 70^\circ\text{C}$	$T_A = 85^\circ\text{C}$
	with ± 15 V	$R_{M\min} = 100 \Omega$	$R_{M\min} = 100 \Omega$
	@ ± 25 At _{max}	$R_{M\max} = 320 \Omega$	$R_{M\max} = 315 \Omega$
	@ ± 36 At _{max}	100	185
I_{SN}	Secondary nominal current rms	25	mA
K_N	Conversion ratio	1-2-3-4-5 : 1000	
V_C	Supply voltage (± 5 %)	± 15	V
I_c	Current consumption	10 + I_s	mA

Accuracy - Dynamic performance data

X	Accuracy @ I_{PN} , $T_A = 25^\circ\text{C}$	± 0.5	%
ε_L	Linearity error	< 0.2	%
I_o	Offset current ¹⁾ @ $I_p = 0$, $T_A = 25^\circ\text{C}$	Typ	Max
I_{OM}	Magnetic offset current ²⁾ @ $I_p = 0$ and specified R_M , after an overload of $3 \times I_{PN}$	± 0.05	± 0.15
I_{OT}	Temperature variation of I_o	mA	mA
	$0^\circ\text{C} .. + 25^\circ\text{C}$	± 0.05	± 0.15
	$+ 25^\circ\text{C} .. + 70^\circ\text{C}$	± 0.06	± 0.25
	$- 25^\circ\text{C} .. + 85^\circ\text{C}$	± 0.10	± 0.35
	$- 40^\circ\text{C} .. + 85^\circ\text{C}$	± 0.5	mA
		± 1.2	mA
t_r	Response time ³⁾ to 90 % of I_{PN} step	< 1	μs
di/dt	di/dt accurately followed	> 50	A/μs
BW	Frequency bandwidth (-1 dB)	DC .. 150	kHz

General data

T_A	Ambient operating temperature	- 40 .. + 85	°C
T_S	Ambient storage temperature	- 45 .. + 90	°C
R_p	Primary coil resistance per turn	@ $T_A = 25^\circ\text{C}$	$< 1.25 \text{ m}\Omega$
R_s	Secondary coil resistance	@ $T_A = 70^\circ\text{C}$	110
		@ $T_A = 85^\circ\text{C}$	115
R_{IS}	Isolation resistance @ 500 V, $T_A = 25^\circ\text{C}$	> 1500	MΩ
m	Mass	22	g
	Standards	EN 50178: 1997	

Notes: ¹⁾ Measurement carried out after 15 mn functioning

²⁾ The result of the coercive field of the magnetic circuit

³⁾ With a di/dt of 100 A/μs.

Features

- Closed loop (compensated) current transducer using the Hall effect
- Isolated plastic case recognized according to UL 94-V0.

Advantages

- Excellent accuracy
- Very good linearity
- Low temperature drift
- Optimized response time
- Wide frequency bandwidth
- No insertion losses
- High immunity to external interference
- Current overload capability.

Applications

- AC variable speed drives and servo motor drives
- Static converters for DC motor drives
- Battery supplied applications
- Uninterruptible Power Supplies (UPS)
- Switched Mode Power Supplies (SMPS)
- Power supplies for welding applications.

Application domain

- Industrial.



VISION MAINTENANCE-FREE
RECHARGEABLE
SEALED LEAD ACID BATTERY*

CP1270 12V 7Ah(20hr)

The rechargeable batteries are lead-lead dioxide systems. The dilute sulfuric acid electrolyte is absorbed by separators and plates and thus immobilized. Should the battery be accidentally overcharged producing hydrogen and oxygen, special one-way valves allow the gases to escape thus avoiding excessive pressure build-up. Otherwise, the battery is completely sealed and is, therefore, maintenance-free, leak proof and usable in any position.



Battery Construction

Component	Positive plate	Negative plate	Container	Cover	Safety valve	Terminal	Separator	Electrolyte
Raw material	Lead dioxide	Lead	ABS	ABS	Rubber	Copper	Fiberglass	Sulfuric acid

General Features

- Absorbent Glass Mat (AGM) technology for efficient gas recombination of up to 99% and freedom from electrolyte maintenance or water adding.
- Not restricted for air transport-complies with IATA/ICAO Special Provision A67.
- UL-recognized component.
- Can be mounted in any orientation.
- Computer designed lead, calcium tin alloy grid for high power density.
- Long service life, float or cyclic applications.
- Maintenance-free operation.
- Low self discharge.

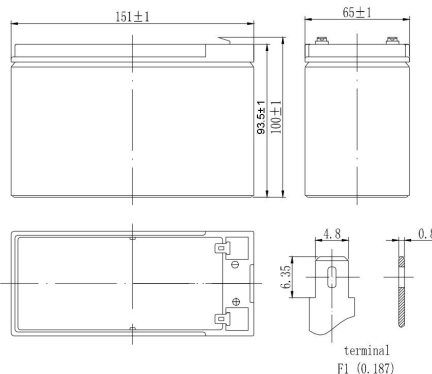
Performance Characteristics

Nominal Voltage	12V
Number of cell	6
Design Life	5 years
Nominal Capacity 77°F(25°C)	
20 hour rate (0.35A, 10.5V)	7Ah
10 hour rate (0.68A, 10.5V)	6.8Ah
5 hour rate (1.13A, 10.5V)	5.65Ah
1 hour rate (4.56A, 9.6V)	4.56Ah
Internal Resistance	
Fully Charged battery 77°F(25°C)	≤ 30mOhms
Self-Discharge	
3% of capacity declined per month at 20°C(average)	
Operating Temperature Range	
Discharge	-20~60°C
Charge	-10~60°C
Storage	-20~60°C
Max. Discharge Current 77°F(25°C)	105A(5s)
Short Circuit Current	350A
Charge Methods: Constant Voltage Charge 77°F(25°C)	
Cycle use	2.40-2.45VPC
Maximum charging current	2.8A
Temperature compensation	-30mV/°C
Standby use	2.23-2.30VPC
Temperature compensation	-20mV/°C

Dimensions and Weight

Length(mm / inch)	151 / 5.94
Width(mm / inch)	65 / 2.56
Height(mm / inch)	93.5 / 3.68
Total Height(mm / inch)	100 / 3.94
Approx. Weight(Kg / lbs)	2.32 / 5.12

* Weight deviation: ± 5%



Discharge Constant Current (Amperes at 77°F25°C)

End Point Volts/Cell	5min	10min	15min	30min	1h	3h	5h	10h	20h
1.60V	29.1	18.4	14.8	8.30	4.56	1.84	1.26	0.70	0.363
1.65V	27.5	17.5	14.2	7.90	4.40	1.80	1.22	0.69	0.359
1.70V	26.0	16.7	13.6	7.62	4.22	1.74	1.17	0.69	0.355
1.75V	24.4	15.7	13.0	7.24	4.04	1.68	1.13	0.68	0.350
1.80V	22.8	14.8	12.4	7.03	3.84	1.63	1.08	0.66	0.344

Discharge Constant Power (Watts at 77°F25°C)

End Point Volts/Cell	5min	10min	15min	30min	45min	1h	2h	3h	5h
1.60V	52.0	35.1	27.5	15.2	11.50	8.97	5.06	3.59	2.33
1.65V	49.4	33.3	26.5	14.6	11.00	8.59	4.94	3.50	2.29
1.70V	46.9	31.6	25.4	14.0	10.50	8.23	4.80	3.40	2.25
1.75V	44.5	29.8	24.3	13.4	10.10	7.99	4.65	3.30	2.21
1.80V	41.6	28.0	23.3	12.9	9.75	7.62	4.50	3.19	2.15

(Note)The above characteristics data are average values obtained within three charge/discharge cycles not the minimum values.

All data shall be changed without notice, Vision reserves the right to explain and update the information contained hereinto.